

# Intracellular lipid in papillary renal cell carcinoma (pRCC): T2 weighted (T2W) MRI and pathologic correlation

Nicola Schieda · Christian B. van der Pol · Bardia Moosavi ·  
Matthew D. F. McInnes · Kien T. Mai · Trevor A. Flood

Received: 14 July 2014 / Revised: 4 January 2015 / Accepted: 16 January 2015 / Published online: 14 February 2015  
© European Society of Radiology 2015

## Abstract

**Objective** To evaluate if pRCCs demonstrate intracellular lipid (i-lipid) at chemical-shift (CS) MRI, and assess T2W-MRI and pathologic characteristics.

**Methodology** Sixty-two patients with a pRCC diagnosis underwent MRI over 11 years (IRB-approved). Two radiologists independently assessed for presence of i-lipid on CS-MRI and homogeneity on T2W-MRI. Inter-observer agreement was assessed via an intraclass correlation and results were compared using the Chi-square test. Discordant cases were reviewed to establish consensus. T2W SI-ratios (SI.tumor/SI.kidney) and CS-SI index were compared using independent t-tests and Spearman correlation. Two pathologists re-evaluated the histopathology.

**Results** Nine of the 62 pRCCs (14.5 %) demonstrated i-lipid; agreement was moderate (ICC=0.63). Pathology review depicted clear cells in four tumours and foamy histiocytes in five tumours.

25.8–35.4 % (ICC=0.65) of tumours were homogeneous on T2W-MRI. No pRCC with i-lipid was considered homogeneous ( $p=0.01$ – $0.04$ ). Overall, T2W SI-ratio and CS-SI index were 0.89 ( $\pm 0.29$ ) and  $-3.63$  % ( $-7.27$  to  $11.42$ ). pRCC with i-lipid had significantly higher T2W SI-ratio ( $p=0.003$ ). There was a correlation between the CS-SI index and T2W SI-ratio, ( $r=0.44$ ,  $p<0.001$ ).

**Conclusions** Intracellular lipid is uncommonly detected in pRCCs due to clear cell changes and foamy histiocytes. These

tumours are associated with heterogeneously-increased SI in T2W-MRI.

## Key Points

- A minority of pRCCs demonstrate intracellular lipid in CS-MRI.
- Quantitatively, intracellular lipid in pRCCs is minimal (<25%).
- Intracellular lipid in pRCCs are from clear cell heterogeneity or foamy histiocytes.
- pRCCs with intracellular lipid are heterogeneously hyperintense at T2W-MRI.
- pRCCs that are homogeneously hypointense at T2W-MRI do not contain intracellular lipid.

**Keywords** Renal cell carcinoma · Clear cell · Papillary · Chemical shift (in and opposed phase) · T2 weighted · Intracellular lipid · Magnetic resonance imaging

## Introduction

Accurate characterization of solid renal masses via imaging is desirable. Renal cell carcinoma (RCC) subtypes (clear cell, papillary and chromophobe) have different biological behaviours [1] and can be accurately differentiated using a combination of imaging findings using magnetic resonance imaging (MRI) [1, 2]. Clear cell RCCs, the most common and most aggressive of the RCC subtypes, is typified by a signal intensity (SI) drop on chemical-shift (CS) in- and opposed-phase MRI due to the presence of intracellular lipid and glycogen within clear cells [2–6]. Clear cell RCC is also characterized by heterogeneously-increased SI on T2-weighted (T2W) imaging [1, 2, 7]. An increased T2W SI is an independent imaging finding recently shown to be highly predictive of

N. Schieda (✉) · C. B. van der Pol · B. Moosavi · M. D. F. McInnes  
Department of Medical Imaging, The Ottawa Hospital,  
The University of Ottawa, 1053 Carling Avenue, Ottawa, Ontario,  
Canada K1Y 4E9  
e-mail: nschieda@toh.on.ca

K. T. Mai · T. A. Flood  
Department of Anatomical Pathology, The Ottawa Hospital,  
The University of Ottawa, Ottawa, Ontario, Canada

malignancy in a solid renal mass [8]. Conversely, papillary RCC (the second most common RCC) is characteristically of low SI on T2W imaging and does not demonstrate i-lipid on CS-MRI [1, 2, 7].

Renal oncocytoma and minimal fat angiomyolipoma (mf-AML) remain commonly resected benign renal neoplasms [9–13]. It is generally accepted that an imaging diagnosis of oncocytoma is currently not possible [14, 15]. Imaging diagnosis of mf-AML remains inconclusive despite a plethora of findings described with both MRI and computed tomography (CT) [5, 7, 8, 16–26]. Low SI on T2W-MRI has been reported in mf-AML [8, 22, 23]; however, this finding overlaps with papillary RCC [1, 7, 8]. A SI drop on CS-MRI (from microscopic fat) in mf-AML [5, 7, 20] is not specific since this imaging finding is also commonly detected in clear cell RCCs [4, 5]. Restricted diffusion with a low apparent diffusion coefficient is a recently described finding in mf-AML [27], but is also characteristic of papillary RCC [28]. Sasiwimonphan et al. previously demonstrated that by combining a SI drop on CS-MRI (excludes papillary RCC) and low T2W SI (excludes clear cell RCC), mf-AML could be diagnosed with a high degree of accuracy [7].

Recently, Karlo et al. described that a SI drop on CS-MRI may be observed not only in clear cell RCC but in all solid renal neoplasms (including papillary RCC) [6]. This observation was speculated to be related to the histopathological heterogeneity of renal tumours (i.e., at histopathology, clear cells can be seen in cortical tumours other than clear cell RCC [29]) and has a major impact on the MR imaging of solid renal masses. This observation could invalidate the supposition that a T2 hypointense renal lesion with an SI drop on CS-MRI probably represents mf-AML and, may also limit the ability of MRI to differentiate papillary from clear cell RCC. The purpose of this study was to validate the observation that papillary RCC may demonstrate a SI drop due to intracellular lipid using chemical shift MRI and to determine if this imaging finding is associated with unique T2W imaging properties. We hypothesized that if papillary RCCs demonstrate intracellular lipid on CS-MRI due to histopathological heterogeneity (the presence of clear cells), these tumours may also resemble clear cell RCC on T2W imaging, demonstrating heterogeneously-increased T2W SI [1]. A secondary objective of this study was to evaluate those papillary RCCs with i-lipid on CS-MRI by histopathology to confirm that: a) the histological classification of papillary RCC was correct; and, b) that clear cells were present within the tumour to account for the SI drop observed on CS-MRI.

## Methodology

### Patient selection

This retrospective cohort study was approved by our research ethics board who waived the need for informed consent.

Between January 2002 and December 2013, we searched the pathology and picture archiving and communication systems (PACS) databases from a single institution for the diagnosis of papillary renal cell carcinoma. Inclusion criteria were as follows: 1) histopathologic diagnosis of papillary RCC from a surgical specimen or biopsy report (reported by subspecialty genito-urinary [GU] pathologists at our institution); and 2) MRI examination including a minimum of chemical shift (in- and opposed-phase) and T2-weighted sequences performed prior to the surgery or biopsy. We identified 75 patients with a histological diagnosis of papillary RCC that underwent MRI. Twelve patients were excluded because: 1) CS-MRI was not performed or severely limited by artefacts (four patients); 2) T2W imaging was not performed (one patient); 3) volume averaging (lesion size was less than half of the slice thickness on chemical shift MRI) (five patients); and, 4) the tumour could not be identified on MRI in two patients with severe autosomal dominant polycystic renal disease. From the 63 patients who met the inclusion criteria, 60 patients had a histopathological diagnosis established from a surgical specimen and three patients had a diagnosis established from 18-gauge core biopsy specimens. One of the 63 patients was re-classified as a clear cell RCC from review of the histopathology and excluded from all further analyses. Therefore, the total study population consisted of 62 patients. There were 22 female patients and the mean age was 63 ( $\pm 12$ ) years.

### MRI technique

In 55 out of 62 patients, MRI was performed at a single tertiary care referral centre using one of three clinical 1.5- or 3-Tesla systems (Magnetom Symphony or TRIO, Siemens Healthcare and Discovery MR750w, General Electric Healthcare) with a torso phased-array coil (8-element anterior array for Discovery, 6-element anterior array for TRIO, and 4-element anterior array for Symphony). In all patients who met the inclusion criteria, breath-hold axial in- and opposed-phase T1W chemical shift gradient recalled echo (GRE) and respiratory-triggered or breath-hold axial T2W turbo spin echo (TSE) or half-Fourier single shot TSE (HASTE, Siemens Healthcare and ssFSE, General Electric Healthcare) sequences were performed. For the T1W dual echo chemical shift GRE sequence, imaging was performed as either a 2-dimensional (2D) (N=37 patients) or 3D sequence (N=18). Prior to 2007, respiratory triggered T2-weighted TSE was performed at 1.5 Tesla (N=37) and after 2005, T2-weighted single shot TSE/FSE (HASTE, Siemens Healthcare and ssFSE, General Electric Healthcare) was performed at both 1.5 and 3 T (N=18). Pulse sequence parameters at 1.5 and 3 T are provided in Table 1.

In the remaining seven patients, MRI was performed at peripheral institutions within our regional Local Hospital

**Table 1** Pulse sequence parameters for dual echo T1 weighted (in- and opposed-phase) GRE and T2-weighted FSE at 1.5 and 3 Tesla<sup>a</sup>

Pulse Sequence	Dual echo T1W GRE			T2W TSE/FSE	
	2D GRE	3D GRE		TSE/FSE	Single shot TSE/FSE
		3 T	1.5 T		
<b>Physiology</b>	Breath Hold	Breath Hold	Breath hold	Respiratory Triggered	Breath hold
<b>Duration</b>	21 sec.	16 sec.	20 sec.	3-4 min.	22 sec.
<b>TE (IP/OP)<sup>b</sup>; TR (msec)</b>	(4.6/2.3); 160-180	(2.5/1.3); 5.5 and (2.2/1.1); 4.0	(4.6/2.3); 7.6	83-92; 5,000	83-88; 1,030
<b>Flip angle (degrees)</b>	70	10 - 12	10	150	180
<b>Bandwidth (Hz)</b>	260	700	313	260	450
<b>Number of excitations</b>	1	0.7 - 1	1	2	Half-Fourier
<b>Acceleration factor</b>	2	2	1	1	2
<b>Matrix Size</b>	256/320 x 134/152	294 x 224	192 x 320	256/320 x 100/132	170 x 256
<b>Field of view (cm)</b>	35	35	35	35	35
<b>Slice thickness (mm)</b>	5 - 6	3 - 4	3 - 5	5	5
<b>Inter-slice gap (mm)</b>	0	0	0	0	0

a- Imaging was performed on a clinical 1.5 Tesla (Symphony or Avanto, Siemens Healthcare; Achieva, Philips Healthcare) or 3 Tesla (TRIO, Siemens Healthcare; Discovery 750 W, General Electric Healthcare) systems.

b- IP=in phase, OP=opposed phase

Integration Network (LHIN) using clinical 1.5-Tesla systems (Avanto, Siemens Healthcare [N=3]; Achieva, Philips Healthcare [N=4]) with studies available for review through our PACS server. A torso phased-array coil was used (6-element array for Avanto and 4-element array for Achieva). The MRI technique was similar to that used at the single tertiary care centre with similar sequence parameters described in Table 1. In all patients, 2D T1W dual echo GRE imaging was performed with a slice thickness of 5 mm. Similarly, in all patients, T2-weighted imaging was performed with a breath-hold single shot rapid acquisition with a relaxation enhancement sequence (HASTE, Siemens Healthcare and Ultrafast spin echo, Philips Healthcare) also using a slice thickness of 5 mm.

#### Visual assessment

Two fellowship-trained abdominal radiologists (NS, MM) with 8 and 14 years of experience, respectively, independently reviewed the T1W dual echo GRE and T2W FSE sequences and assessed the following: A) the presence of intracellular lipid (defined as a region of visual SI drop within the tumour on opposed-phase [OP] compared to in-phase [IP] images); and, B) homogeneity of the tumour on T2W imaging. Intracellular lipid and homogeneity were defined as binary outcomes (i.e., present or absent, and homogeneous or heterogeneous). After the initial independent review sessions, both radiologists reviewed the discordant cases of intracellular lipid in tandem to establish a consensus diagnosis.

#### Quantitative assessment

Twelve weeks after the consensus review was performed, a radiology resident (CV) and one of the abdominal radiologists (NS) measured the size of each tumour in the anterior-posterior, transverse and cranio-caudal dimensions (mm) and the mean was recorded. The SI on both T1W dual echo GRE and T2W FSE sequences were recorded. On chemical shift (IP and OP) sequences, a circular region of interest (ROI) was placed within the tumour (in the same location on both IP and OP), encompassing at least two thirds of the solid component, as described previously [5]. The periphery of the tumour, renal hilum and spleen were avoided to prevent erroneously decreased values on OP images from a phase cancellation artefact where the tumour interfaced with retroperitoneal or renal sinus fat [5]. On T2W imaging, when the tumour was heterogeneous, an ROI was placed in the most T2 hyperintense solid region (excluding areas of necrosis and cystic change by correlation with contrast enhanced imaging sequences). If the tumour was homogeneous, the ROI was measured within the centre of the renal mass. The mean ROI area for T2 measurements was 30.8 ( $\pm$ 20.7) mm<sup>2</sup>. On T2W FSE images, the same-sized ROI (as used to measure the SI of the tumour) was placed in the ipsilateral renal cortical parenchyma (avoiding the edge of the kidney and renal sinus), as described previously [7]. For the chemical shift MRI, an SI index for each tumour was calculated according to the following equation:  $[(SI_{\text{tumourIP}} - SI_{\text{tumourOP}})/SI_{\text{TumourIP}}] \times 100$  [5–7]. For the T2-weighted MRI, a tumour-to-renal cortical parenchyma (herein referred to as

tumour-to-cortex) SI ratio was calculated according to the following equation:  $SI_{\text{tumour}}/SI_{\text{Cortex}}$  [7].

### Histopathological assessment

The histopathological diagnosis of papillary RCC for the 63 patients included in the study were retrieved from surgical (N=60) or core biopsy (N=3) reports. After the radiologist's visual assessment and consensus review, tumours with intracellular lipid detected via CS-MRI were independently re-reviewed by two GU pathologists (TF, KM) with 8 and 35 years of experience in GU pathology, respectively. The pathologists were instructed to evaluate each tumour and to: a) determine the classification of the tumour (clear cell, papillary, chromophobe or mixed features) and, b) assess for the presence of clear cells, adipocytes or other fat-containing structures that could potentially account for the observed SI drop in CS-MRI. Tumours were classified according to the following morphological criteria: a) for clear cell RCCs, tumour cells were arranged in sheets, nests, acini, microcystic or macrocystic structures. Malignant cells typically showed optically clear cytoplasm (due to the loss of cytoplasmic lipids and glycogen during histologic processing) and were separated by numerous thin-walled blood vessels. [30]; b) for papillary RCCs, tumours were composed of variable amounts of papillae, tubulopapillae, and tubules. The papillae contained fibrovascular cores. The neoplastic cells lining the papillae were typically arranged in a single layer but were occasionally pseudostratified. The cytoplasm was pale or densely eosinophilic, or clear [31–33]; and, c) for chromophobe RCCs, malignant cells were typically arranged in sheets intersected by medium-caliber blood vessels [34]. Large polygonal cells with prominent “plant cell-like” cell membranes were seen and the nuclei were irregular and wrinkled; perinuclear halos are frequently seen. (5) When tumours demonstrated features of more than one subtype, this was also recorded.

### Statistical analysis

The incidence of intracellular lipid detected subjectively with CS-MRI was calculated for each reader. Similarly, the incidence of T2W heterogeneity was determined for each reader. Inter-observer agreement was assessed using an intraclass correlation coefficient (ICC), where: 0 - 0.2 indicates *poor* agreement; 0.3 - 0.4 indicates *fair* agreement; 0.5 - 0.6 indicates moderate agreement; 0.7 - 0.8 indicates *strong* agreement; and >0.8 indicates *almost perfect* agreement. To determine the association between the subjective assessment of intracytoplasmic lipid (after consensus review) and the T2W tumour heterogeneity, a Chi square test was performed.

All parametric data is presented as the mean ( $\pm$  standard deviation) unless the data is skewed, in which case the median (interquartile range) is reported. A Spearman correlation was

performed to determine the association between the chemical shift SI index and the T2W SI ratios. T2W SI ratios for tumours with intra-cellular lipid were compared using an independent t-test.

A threshold *p* value < 0.05 was considered to indicate a statistically significant difference. Statistical analysis was performed with STATA data analysis and statistical software, version 13.

### Results

Results for the subjective assessment of intracellular lipid content and T2W heterogeneity are provided in Table 2. Reader 1 identified intracellular lipid in 22.6 % (14/62) of the pRCCs and Reader 2 identified 9.7 % (6/62). Inter-observer agreement was moderate (ICC=0.63). After consensus review, 14.5 % (9/62) of the pRCCs contained intracellular lipid.

Papillary RCCs with intracellular lipid were re-evaluated by two GU pathologists. Both pathologists re-classified one of the papillary RCCs with intracellular lipid as a clear-cell RCC; this tumour was excluded from all analyses. In four of the nine pRCCs, clear cells were identified in the tumour, but other typical morphological features of papillary RCCs were identified by both pathologists (Fig. 1). In the other five cases, a diagnosis of papillary RCC was confirmed by both pathologists who determined that either no clear cells or only a trace amount of clear cells were present. In all five of these cases, both pathologists identified large amounts of foamy lipid-laden histiocytic cells arranged either in aggregates or in papillary tips (Fig. 2) as the probable cause for the SI drop in CS-MRI.

A homogeneous T2W SI was observed in 25.8 - 35.4 % of tumours overall (ICC=0.65). T2W imaging characteristics for those pRCCs with intracellular lipid are provided in Table 3. All pRCCs with intracellular lipid were considered heterogeneous on T2W imaging by both readers and at consensus review (Figs. 1 and 2). Similarly, no papillary RCC that was homogeneous on T2W imaging demonstrated intracellular lipid at chemical-shift MRI (Fig. 3). There was an association

**Table 2** Subjective assessment of intracellular lipid content on T1 weighted (T1W) dual echo gradient recalled echo and T2W homogeneity on T2-weighted (T2W) fast spin echo MRI in papillary renal cell carcinomas

	Intracellular Lipid		Homogeneity on T2W MRI	
	Present	Absent	Homo- geneous	Hetero- geneous
Reader 1	14	48	22	40
Reader 2	6	56	16	46
ICC <sup>a</sup>	0.63		0.65	

<sup>a</sup> ICC=intraclass correlation coefficient.



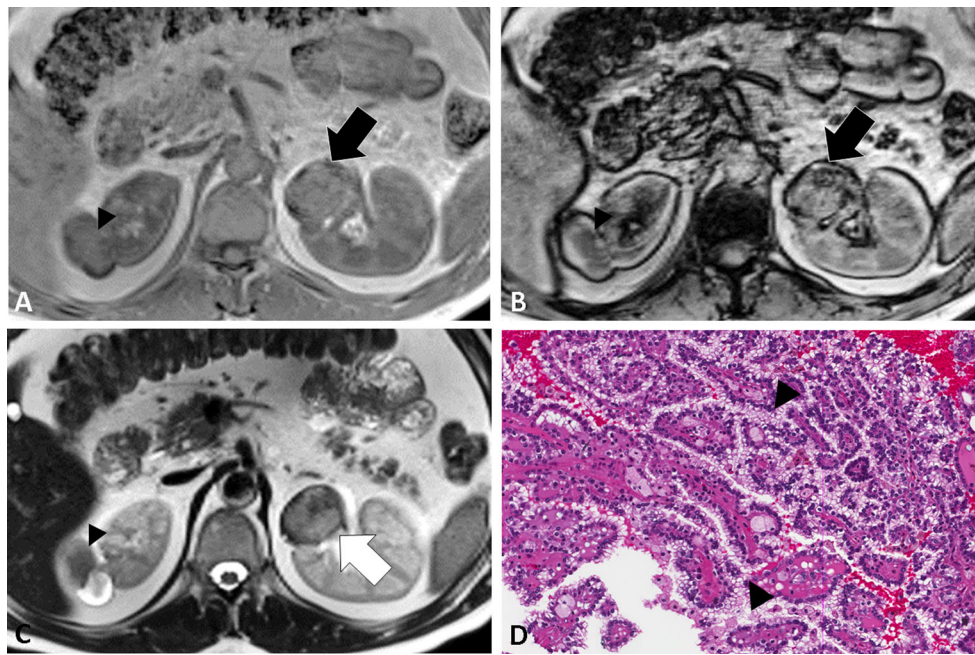


**Fig. 1** 56-year-old female patient with papillary renal cell carcinoma (pRCC). Axial T1 weighted (T1W) dual echo (in- [a] and opposed-phase [b]) gradient recalled echo (GRE) images demonstrate the presence of focal signal intensity drop within the pRCC (black arrows); note signal intensity drop on opposed-phase (b) compared to in-phase (a) images. The chemical shift signal intensity (SI) index was 14 %. Axial T2-weighted (T2W) single shot fast spin echo (ssFSE) image (c)

demonstrates heterogeneously increased signal (white arrow). The corresponding microscopic image (e) demonstrates pRCC features with papillae lined by neoplastic cells with clear cytoplasm (black arrowheads). Also, note the presence of a more typical pRCC in the contralateral kidney (partially included) with no SI drop on OP imaging and homogeneously low T2W signal intensity (arrowheads) cranial to a benign renal cyst (in a-c)

between T2 heterogeneity and the presence of intracellular lipid for both readers ( $p=0.01 - 0.04$ ).

The median CS-SI index  $(((SI.IP-SI.OP)/SI.IP) \times 100)$  overall was  $-3.63\%$  (range,  $-7.27 - 11.42$ ). For those tumours that demonstrated intracellular lipid subjectively, the mean CS-SI index was  $16.34\%$  ( $\pm 9.67$ ) and the range was  $8.2 -$

$19.8\%$ . The tumour that was re-classified as a clear cell RCC demonstrated a SI index of  $41.9\%$ . For the remaining 53 tumours that did not demonstrate intracellular lipid subjectively, the mean CS-SI index was  $-7.33$  (range,  $-8.88 - 8.63$ ). There was a difference in the CS-SI index between tumours with intracellular lipid subjectively and those without ( $p=$

**Fig. 2** 63-year-old male with a pRCC. Axial T1W dual echo (in- [a] and opposed-phase [b]) GRE demonstrate a diffuse signal intensity drop on opposed-phase (b) compared to in-phase (a) images (black arrows). The chemical shift signal intensity (SI) index was 16 %. Axial T2W single shot ssFSE image (c) demonstrates heterogeneously increased T2W internal signal (white arrow). The corresponding microscopic image (d) demonstrates pRCC features with the tips of the papillae distended by macrophages containing abundant foamy cytoplasm

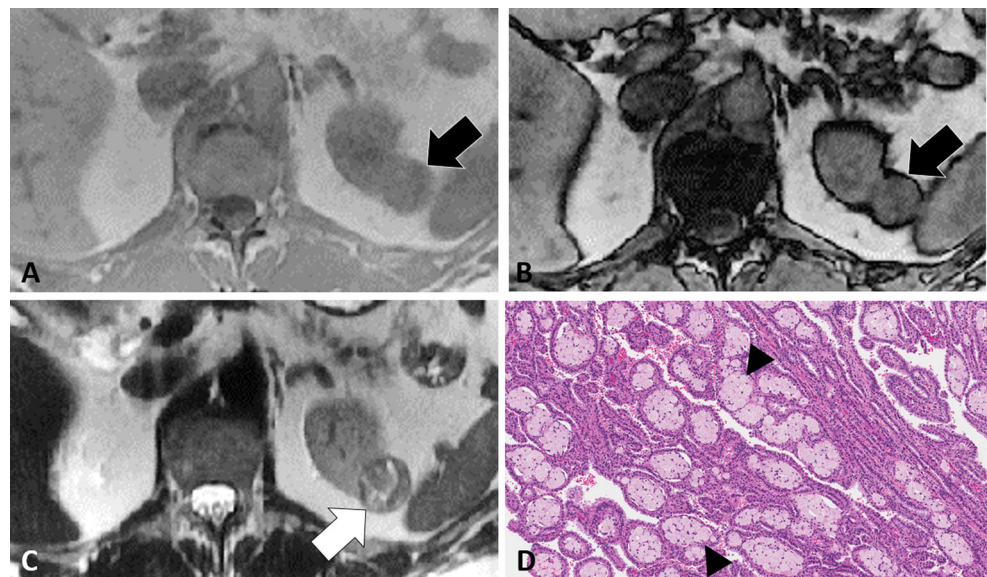


**Table 3** T2W homogeneity of papillary renal cell carcinomas demonstrating intracellular lipid at T1W dual echo gradient recalled echo MRI (determined by subjective assessment)

Intracellular lipid present in tumour	T2W Homogeneity	
	Homogeneous	Heterogeneous
Reader 1	0	14
Reader 2	0	6
Consensus <sup>a</sup>	0	9
Reader 1	0	9
Reader 2	0	9

a- Consensus diagnosis was established by tandem review of discordant cases by both readers after an independent analysis

0.04). The mean T2W SI ratio (relative to the renal cortex) overall was 0.88 ( $\pm 0.29$ ). There was a significant positive correlation between the CS-SI index and T2W SI ratio ( $r=0.44$ ,  $p<0.001$ ; Fig. 4). There was a difference in the mean T2W SI ratio for those tumours with intracellular lipid ( $1.23\pm 0.32$ ) compared to those tumours without intracellular lipid ( $0.81\pm 0.23$ ,  $p=0.003$ ; Fig. 5).

**Discussion**

Our study validates the recently described observation by Karlo et al. that papillary RCCs may demonstrate intracellular lipid on chemical shift MRI [6]. In this study, using a similar methodology, 14.5 % of papillary RCCs demonstrated intracellular lipid subjectively (after consensus review), which is comparable to the 17 – 29 % rate reported by Karlo et al. [6]. The mean chemical shift SI index for those tumours that visually demonstrated intracellular lipid was 16.34 %, which compares favourably to the 8 - 11.6 % reported by Karlo et al. [6]. The overall CS-SI index in our study (-3.63 %) also compares favourably to the CS-SI index for pRCCs (-6.1 %) reported in the recent study by Cornelis et al. [2]. Karlo et al. previously reported that by using a CS-SI index threshold of 25 %, clear cell RCCs with intra-cellular lipid could be differentiated from other tumours with intra-cellular lipid (including papillary

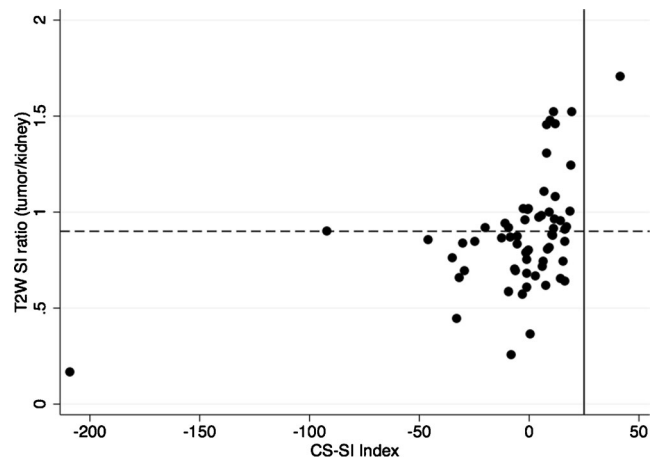


**Fig. 4** Scatter plot of T2W signal intensity (SI) ratio and chemical shift (CS) SI index illustrating the positive association between the T2W SI ratio and the CS-SI index observed in this study. Only one tumour demonstrated a CS-SI index above 25 % (solid black line) and this tumour was re-classified as a clear cell RCC. There were no tumours with a CS-SI index >20 % that demonstrated a T2W SI ratio <0.9 (dotted black line), thresholds previously described used to differentiate minimal fat AML from RCC [7]

RCCs) [6]. Our study confirms that papillary RCCs with intracellular lipid demonstrate a mild SI drop (less than 25 %). In this study, only a single tumour had a CS-SI index above 25 % and this was re-classified as a clear cell RCC at histopathological review. The inter-observer agreement in this study was moderate, which compares favourably to the “fair” inter-observer agreement observed by Karlo et al. [6]. This result supports the conclusion by these authors that when an SI drop in chemical shift imaging is mild (CS-SI index < 25 %), the inter-observer agreement for the finding will decrease.

In this study, all papillary RCCs that demonstrated intracellular lipid were subjectively considered heterogeneous and demonstrated a higher T2W SI when compared to those papillary RCCs without intracellular lipid. To our knowledge, this observation is previously unreported. Our overall T2W SI ratio for papillary RCCs compares favourably to that reported previously (0.70) by Cornelis et al. [2].

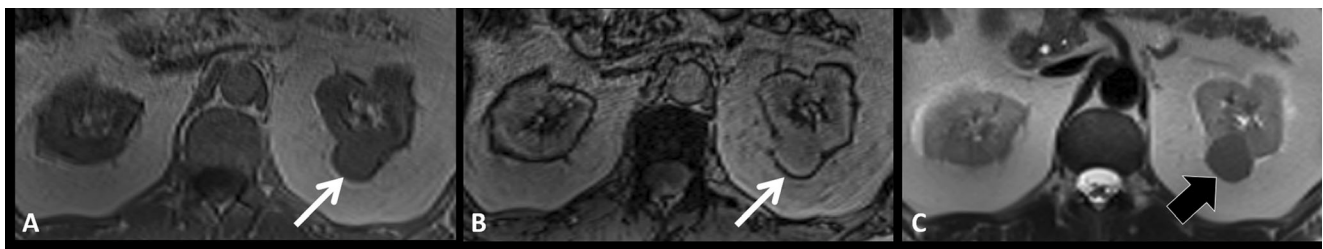


**Fig. 3** Axial in-phase (a) and opposed-phase (b) T1W GRE images in a 46-year-old female patient with a pRCC (white arrows) with no signal intensity drop (no intracellular lipid), demonstrates a homogeneously low

T2 signal intensity mass on the axial T2W ssFSE image (black arrow in c). In this study, there were no tumours with homogeneously low T2W signal intensity which also demonstrated intracellular lipid at chemical shift MRI

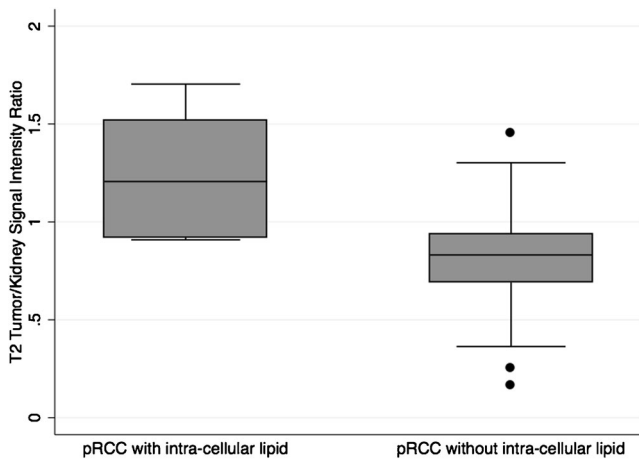


**Fig. 5** Box and whisker plots illustrating the association between T2W signal intensity (SI) ratio and the presence of intra-cellular lipid on CS-MRI. A papillary RCC with intracellular lipid had a significantly higher T2W SI ratio compared to tumours without intracellular lipid,  $p=0.003$

Karlo et al. speculated that the observation of intracellular lipid in non-clear cell RCC was related to the histopathological finding of clear cell heterogeneity, which is the presence of clear cells in other RCC subtypes [6]. A limitation of their study was that histopathologic review of the tumours with intracellular lipid detected using MRI was not performed. It could be argued that the uncommon finding of a SI drop in CS-MRI in non-clear cell tumours may be related to the presence of small amounts of intra-tumoral adipocytes (different from intracellular lipids), which has been described in papillary RCCs [35, 36]. Furthermore, the distinction between papillary and clear cell tumours can be occasionally challenging and it is possible that the subset of papillary RCCs with intracellular lipid in the study by Karlo et al. were misclassified clear cell RCCs, mixed papillary-clear cell RCCs or clear-cell tubulopapillary RCCs [37–39]. In order to expand upon the observations by Karlo et al., we performed a histopathological review of all cases of papillary RCCs with intracellular lipid detected via CS-MRI. In our study, one tumour was reclassified as a clear cell RCC and four of nine tumours demonstrated clear cells in the background of otherwise typical papillary RCC features. In the remaining five tumours, clear cells were either absent or only present in trace amounts and not likely to be the cause of any SI drop on CS-MRI. In those tumours, large aggregates of foamy lipid-laden histiocytes were present and likely accounted for the observed SI drop on CS-MRI. Our findings could potentially explain why the CS-SI index in papillary tumours with intracellular lipid is less than what has been reported in clear cell tumours; it is either related to an admixture of less clear cells or a reduced concentration of lipids in foamy histiocytes as compared to clear cells.

Our study has important application in clinical practice. First, our study confirms the observation by Karlo et al. that a minority of papillary RCCs can demonstrate intracellular lipid on CS-MRI and that, in these tumours, the SI drop is

mild (less than 25 %). More importantly, our study demonstrates that papillary RCCs with intracellular lipid are heterogeneously hyperintense on T2W MRI. Previously, Sasiwimonphan et al. demonstrated that by using a chemical shift SI index threshold of 20 % and a T2W SI ratio of 0.9, minimal fat AML could be differentiated from RCC [7]. Our results support this conclusion; in this study, there were no papillary RCCs with a CS-SI index above 20 % with a T2W SI ratio less than 0.9.

The main limitation of this study is heterogeneity of the study population and the differing MRI protocols used to image renal masses during the study period. Specifically, a combination of 2D and 3D GRE was used for in- and opposed-phase imaging and examinations were performed at 1.5 and 3 Tesla. Similarly, T2-weighted imaging was performed using a combination of respiratory triggered fast spin echo (FSE) and breath hold half Fourier single shot FSE. We feel this is an expected limitation given the large study period we selected in order to include as many papillary RCCs as possible. The lack of a multi-parametric (mp) MRI protocol is another limitation of this study that can be expected since mp-MRI of renal masses has only recently become the reference standard for renal mass MRI [2, 28, 40, 41]. We did not assess whether those papillary tumours with intracellular lipid demonstrated differing imaging characteristics on diffusion-weighted imaging or dynamic contrast enhancement and this will require further study. Another limitation of this study is that we did not compare our results to clear cell RCCs or minimal fat AML in MRI. We feel this is a minor limitation given these comparisons have been performed previously in well designed studies [2, 5–7] using an MRI technique similar to our study and that the primary purpose of this study was to assess the chemical shift and T2-weighted imaging characteristics of papillary RCCs only.

In conclusion, this study confirms the finding of intracellular lipid in a minority of papillary renal cell cancers using chemical shift MRI, which is due to clear cell changes or aggregates of foamy histiocytes. Papillary cancers containing intracellular lipid demonstrate a mild SI drop with a chemical shift SI index of less than 25 %. Papillary RCCs with intracellular lipid demonstrate heterogeneously increased SI on T2W MRI. In this study, using previously described imaging criteria for the diagnosis of minimal fat AML (combination of homogeneously low T2W SI and SI drop in chemical shift MRI) all papillary RCCs would have been correctly diagnosed.

**Acknowledgements** The scientific guarantor of this publication is Nicola Schieda, MD. The authors of this manuscript declare no relationships with any companies whose products or services may be related to the subject matter of the article. The authors state that this work has not received any funding. Nicola Schieda MD, has significant statistical expertise. Institutional Review Board approval was obtained. Written



informed consent was waived by the Institutional Review Board. Methodology: retrospective, cross sectional study, performed at one institution.

## References

- Pedrosa I, Sun MR, Spencer M et al (2008) MR imaging of renal masses: correlation with findings at surgery and pathologic analysis. *Radiographics* 28:985–1003
- Comelis F, Tricaud E, Lasserre AS et al (2014) Routinely performed multiparametric magnetic resonance imaging helps to differentiate common subtypes of renal tumours. *Eur Radiol* 24:1068–1080
- Beddy P, Genega EM, Ngo L et al (2014) Tumor necrosis on magnetic resonance imaging correlates with aggressive histology and disease progression in clear cell renal cell carcinoma. *Clin Genitourin Cancer* 12:55–62
- Outwater EK, Bhatia M, Siegelman ES, Burke MA, Mitchell DG (1997) Lipid in renal clear cell carcinoma: detection on opposed-phase gradient-echo MR images. *Radiology* 205:103–107
- Hindman N, Ngo L, Genega EM et al (2012) Angiomyolipoma with minimal fat: can it be differentiated from clear cell renal cell carcinoma by using standard MR techniques? *Radiology* 265:468–477
- Karlo CA, Donati OF, Burger IA et al (2013) MR imaging of renal cortical tumours: qualitative and quantitative chemical shift imaging parameters. *Eur Radiol* 23:1738–1744
- Sasiwimonphan K, Takahashi N, Leibovich BC, Carter RE, Atwell TD, Kawashima A (2012) Small (<4 cm) renal mass: differentiation of angiomyolipoma without visible fat from renal cell carcinoma utilizing MR imaging. *Radiology* 263:160–168
- Chung MS, Choi HJ, Kim MH, Cho KS (2014) Comparison of t2-weighted MRI with and without fat suppression for differentiating renal angiomyolipomas without visible fat from other renal tumors. *AJR Am J Roentgenol* 202:765–771
- Frank I, Blute ML, Cheville JC, Lohse CM, Weaver AL, Zincke H (2003) Solid renal tumors: an analysis of pathological features related to tumor size. *J Urol* 170:2217–2220
- Remzi M, Ozsoy M, Klingler HC et al (2006) Are small renal tumors harmless? Analysis of histopathological features according to tumors 4 cm or less in diameter. *J Urol* 176:896–899
- Violette P, Abourbih S, Szymanski KM et al (2012) Solitary solid renal mass: can we predict malignancy? *BJU Int* 110:E548–552
- Fujii Y, Komai Y, Saito K et al (2008) Incidence of benign pathologic lesions at partial nephrectomy for presumed RCC renal masses: Japanese dual-center experience with 176 consecutive patients. *Urology* 72:598–602
- Kutikov A, Fossett LK, Ramchandani P et al (2006) Incidence of benign pathologic findings at partial nephrectomy for solitary renal mass presumed to be renal cell carcinoma on preoperative imaging. *Urology* 68:737–740
- Rosenkrantz AB, Hindman N, Fitzgerald EF, Niver BE, Melamed J, Babb JS (2010) MRI features of renal oncocytoma and chromophobe renal cell carcinoma. *AJR Am J Roentgenol* 195:W421–427
- Schieda N, McInnes MD, Cao L (2014) Diagnostic accuracy of segmental enhancement inversion for diagnosis of renal oncocytoma at biphasic contrast enhanced CT: systematic review. *Eur Radiol*
- Yang CW, Shen SH, Chang YH et al (2013) Are there useful CT features to differentiate renal cell carcinoma from lipid-poor renal angiomyolipoma? *AJR Am J Roentgenol* 201:1017–1028
- Schieda N HT, El-Khodary M, McInnes MDF (2014 (In Press)) Non-contrast enhanced computed tomography (NECT) for the diagnosis of minimal fat renal angiomyolipoma (AML). *American Journal of Roentgenology*
- Israel GM, Hindman N, Hecht E, Krinsky G (2005) The use of opposed-phase chemical shift MRI in the diagnosis of renal angiomyolipomas. *AJR Am J Roentgenol* 184:1868–1872
- Vargas HA, Chaim J, Lefkowitz RA et al (2012) Renal cortical tumors: use of multiphasic contrast-enhanced MR imaging to differentiate benign and malignant histologic subtypes. *Radiology* 264:779–788
- Kim JK, Kim SH, Jang YJ et al (2006) Renal angiomyolipoma with minimal fat: differentiation from other neoplasms at double-echo chemical shift FLASH MR imaging. *Radiology* 239:174–180
- Kim JY, Kim JK, Kim N, Cho KS (2008) CT histogram analysis: differentiation of angiomyolipoma without visible fat from renal cell carcinoma at CT imaging. *Radiology* 246:472–479
- Jinzaki M, Tanimoto A, Narimatsu Y et al (1997) Angiomyolipoma: imaging findings in lesions with minimal fat. *Radiology* 205:497–502
- Choi HJ, Kim JK, Ahn H, Kim CS, Kim MH, Cho KS (2011) Value of T2-weighted MR imaging in differentiating low-fat renal angiomyolipomas from other renal tumors. *Acta Radiol* 52:349–353
- Chaudhry HS, Davenport MS, Nieman CM, Ho LM, Neville AM (2012) Histogram analysis of small solid renal masses: differentiating minimal fat angiomyolipoma from renal cell carcinoma. *AJR Am J Roentgenol* 198:377–383
- Catalano OA, Samir AE, Sahani DV, Hahn PF (2008) Pixel distribution analysis: can it be used to distinguish clear cell carcinomas from angiomyolipomas with minimal fat? *Radiology* 247:738–746
- Schieda N, Avruch L, Flood TA (2014) Small (<1 cm) incidental echogenic renal cortical nodules: chemical shift MRI outperforms CT for confirmatory diagnosis of angiomyolipoma (AML). *Insights Imaging*
- Tanaka H, Yoshida S, Fujii Y et al (2011) Diffusion-weighted magnetic resonance imaging in the differentiation of angiomyolipoma with minimal fat from clear cell renal cell carcinoma. *Int J Urol* 18:727–730
- Lassel EA, Rao R, Schwenke C, Schoenberg SO, Michaely HJ (2014) Diffusion-weighted imaging of focal renal lesions: a meta-analysis. *Eur Radiol* 24:241–249
- Reuter VE (2006) The pathology of renal epithelial neoplasms. *Semin Oncol* 33:534–543
- Eble JN SG, Epstein JI, Sesterhenn IA (2004) World Health Organization classification of tumors: Pathology and genetics of tumors of the urinary system and male genital organs. Lyon, Fr. Available via <http://www.iarc.fr/en/publications/pdfs-online/pat-gen/bb7/BB7.pdf2013>
- Delahunt B, Eble JN (1997) Papillary renal cell carcinoma: a clinicopathologic and immunohistochemical study of 105 tumors. *Mod Pathol* 10:537–544
- Lefevre M, Couturier J, Sibony M et al (2005) Adult papillary renal tumor with oncocytic cells: clinicopathologic, immunohistochemical, and cytogenetic features of 10 cases. *Am J Surg Pathol* 29:1576–1581
- Renshaw AA, Corless CL (1995) Papillary renal cell carcinoma. Histology and immunohistochemistry. *Am J Surg Pathol* 19:842–849
- Thoenes W, Storkel S, Rumpelt HJ, Moll R, Baum HP, Werner S (1988) Chromophobe cell renal carcinoma and its variants—a report on 32 cases. *J Pathol* 155:277–287
- Garin JM, Marco I, Salva A, Serrano F, Bondia JM, Pacheco M (2007) CT and MRI in fat-containing papillary renal cell carcinoma. *Br J Radiol* 80:e193–195
- Schuster TG, Ferguson MR, Baker DE, Schaldenbrand JD, Solomon MH (2004) Papillary renal cell carcinoma containing fat without



- calcification mimicking angiomyolipoma on CT. *AJR Am J Roentgenol* 183:1402–1404
37. Mai KT, Faraji H, Desantis D, Robertson SJ, Belanger EC, Levac J (2010) Renal cell carcinoma with mixed features of papillary and clear cell cytology: a fluorescent in situ hybridization study. *Virchows Arch* 456:77–84
  38. Mai KT, Kohler DM, Roustan Delatour NL, Veinot JP (2006) Cytohistopathologic hybrid renal cell carcinoma with papillary and clear cell features. *Pathol Res Pract* 202:863–868
  39. Aydin H, Chen L, Cheng L et al (2010) Clear cell tubulopapillary renal cell carcinoma: a study of 36 distinctive low-grade epithelial tumors of the kidney. *Am J Surg Pathol* 34:1608–1621
  40. Campbell N, Rosenkrantz AB, Pedrosa I (2014) MRI phenotype in renal cancer: is it clinically relevant? *Top Magn Reson Imaging* 23: 95–115
  41. Ramamurthy NK MB, McInnes MDF, Flood TA, Schieda N (2014) Multi-parametric (MP) MRI of solid renal masses: Pearls and Pifalls. *Clinical Radiology*